A Fundamental Study of Applying Wind Turbines for Power System Frequency Control

Felipe Wilches-Bernal, *Student Member, IEEE*, Joe H. Chow, *Fellow, IEEE*, and Juan J. Sanchez-Gasca, *Fellow, IEEE*

***Abstract*—As wind penetration increases in power systems around the world, new challenges to the controllability and operation of a power system are encountered. In particular, frequency response is impacted when a considerable amount of power-electronics interfaced generation, such as wind, is connected to the system. This paper uses small-signal analysis and dynamic simulation to study frequency response in power systems and investigate how Type-3 DFAG wind turbines can impact this response on a test power system, whose frequency response is determined mainly by a *frequency-regulation mode*. By operating the wind turbines in a deloaded mode, a proposed pitch-angle controller is designed using a root-locus analysis. Time simulations are used to demonstrate the transient and steady-state performance of the proposed controller in the test system with 25% and 50% wind penetration.**

***Index Terms*—DFAG wind turbine, frequency response, linear analysis, pitch angle control, root-locus analysis, wind generation.**

I. Introduction

THE installed capacity of wind generation in power systems around the world has experienced an upward trend during the past decade and the growth is expected to continue. In the US, wind generation capacity has represented 33% of all capacity additions since 2007. States like Iowa and South Dakota have a percentage of in-state generation due to wind above 25% and the nationwide total was about 4.1% by the end of 2013 [1]. The total installed wind-turbine (WT) capacity in the US by the end of 2013 was over 61.1 GW with more than 12 000 MW under construction [2].

This reality poses new challenges for the operation of power systems mainly because wind power plants interact differently with the grid. In particular, system frequency response would decrease as the power-electronics interface decouples the WT rotor inertias from the grid [3], [4].

Manuscript received October 25, 2014; revised February 05, 2015 and April 06, 2015; accepted May 07, 2015. This work was supported in part by the Global Climate and Energy Project (GCEP) from Stanford University and in part by the Engineering Research Center Program of the National Science Foundation and the Department of Energy under NSF Award Number EEC-1041877 and the CURENT Industry Partnership Program. Paper no. TPWRS-01482-2014.

F. Wilches-Bernal and J. H. Chow are with the Department of Electrical, Computer, and Systems Engineering, Rensselaer Polytechnic Institute, Troy, NY 12180 USA (e-mail: wilchf@rpi.edu; chowj@rpi.edu).

J. J. Sanchez-Gasca is with GE Energy Consulting, Schenectady, NY 12345 USA (e-mail: juan1.sanchez@ge.com).

Color versions of one or more of the figures in this paper are available online at http://ieeexplore.ieee.org.

Digital Object Identifier 10.1109/TPWRS.2015.2433932

A. Related Work

Various approaches have been proposed in the literature to enable frequency regulation in wind turbine generators (WTGs). These methods can be roughly divided in two categories: those that emulate inertial response by extracting extra power from the WT rotor inertia should a frequency drop occurs and those that deload the wind turbine to provide headroom for frequency regulation.

The investigations in [5]–[12] provide inertial response by changing the torque setpoint to release the rotor kinetic energy, allowing the WT rotor speed to decrease. This control action reduces the frequency dip and the rate of change of frequency [6], [7]. However, the extra power provided by this inertia emulation approach is only temporary for up to 10 s, and does not impact the steady-state frequency [13].

Frequency regulation results falls mainly into two groups:

1) deloading of the WTs by pitching the rotor blade angle [14]–[17], and
2) operating the wind units at a suboptimal rotor speed for maximum energy capture [15]–[22].

The droop settings in most of these investigations are based on prespecified droop schedules. Deloading of WTs is not practiced currently due to potential loss of revenue. However, because interconnection standards are starting to require wind generation to provide frequency response the same way conventional generation does [23]–[26], deloading may be an option for wind energy producers to comply with these requirements. In addition, the loss in revenue can be compensated by enabling the WTGs to participate in the frequency regulation market [27]. Thus the results in this paper pertain to the latter case.

B. Approach and Contributions

This paper provides a systematic investigation on the design of Type-3 DFAG wind turbine blade pitch control for frequency regulation response in a 4-machine power system and a larger 10-machine system. The proposed blade pitch controller consists of two parts: 1) a frequency droop control similar to the governing function in a steam turbine, and 2) a transient gain controller similar to the inertia emulation function [28] to enhance the initial response. Such a two-part controller for WTs has also been proposed in [29]. The contributions of this paper include:

1) The proposed controller can be readily implemented on existing WTG controllers, without requiring additional actuators. It uses the frequency deviation to update the WTG power order to command the existing blade pitch controller to adjust the pitch angle.

2) The proposed controller can operate with a variable headroom and does not rely on a fixed droop schedule.
3) WT simulation studies are supplemented by analysis on a linearized model of the nonlinear power system and WTs, allowing a root-locus analysis to be performed for tuning the controller gains.
4) The control design is based on the frequency regulation mode in the test system, which is tuned to resemble US power grid frequency response.
5) The WT frequency regulation performance is verified for 50% wind penetration.
6) The proposed controller shows good frequency regulation performance in wind perturbation analysis and for a realistic wind profile.

C. Outline

This paper is organized as follows. Sections II and III outline the conventional approach to frequency control and the effects of integrating wind with 25% penetration, respectively, on a test system. Section IV describes a method for enabling frequency response in WTs. Section V presents the proposed control in an increased penetration level of 50%. Finally, conclusions and future work are stated in Section VI.

II. Frequency Control Overview

Frequency must be kept in a tight range for a power system to operate efficiently and reliably. It is a global variable such that generation-load imbalance is visible throughout the entire grid. In order to regulate frequency, power system operators need both controllable generation and load to react to changes in generation or load. The control actions are usually applied in different stages and time frames in a control continuum [30] as described in Table I. The rows in Table I correspond to classifications on how the generation and load should respond and the appropriate time frame.

This paper addresses the primary frequency control (or frequency response) which is provided by generators adjusting their power production due to governing actions and load changes.

A. Frequency Response Characteristics

Fig. 1 shows a typical response of the primary frequency control of a power system for a loss-of-generation event. The most important factors to take into account in the frequency response are:

- **Rate of Change of Frequency (RoCoF)**—a factor that determines how fast the frequency is decreasing and should not be above certain limits as strong decelerations may be deleterious for generators [31].
- **Frequency nadir**—the maximum frequency excursion before frequency starts to recover, which is determined by the frequency difference between Points A and C in Fig. 1.
- **Settling frequency**—Point B in Fig. 1 is the frequency to which the primary frequency control stabilizes.

An important parameter describing the frequency response of the system is Beta (β) or the stiffness of the system [32]. It is the rate of change in generation (or load) with respect to the resulting change in frequency. A higher value of β translates into a smaller frequency change for the same load or generation disturbance. The measured value of β is reported to have decreased in the Eastern Interconnection [33] and in the Texas Interconnect [34].

TABLE I
Control Continuum (Taken From [30, Table 1])

Control	Ancillary Service	Time frame
Primary Control	Frequency Response	10-60 Seconds
Secondary Control	Regulation	1-10 Minutes
Tertiary Control	Imbalance/Reserves	10 Minutes - Hours
Time Control	Time Error Correction	Hours

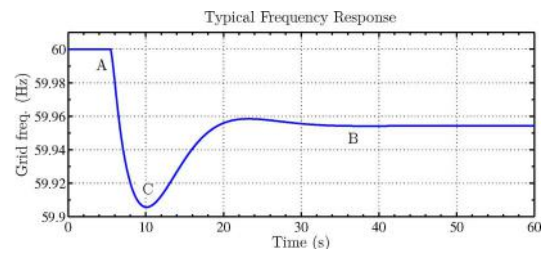

Fig. 1. Typical frequency excursion of a power system for a loss of generation event.

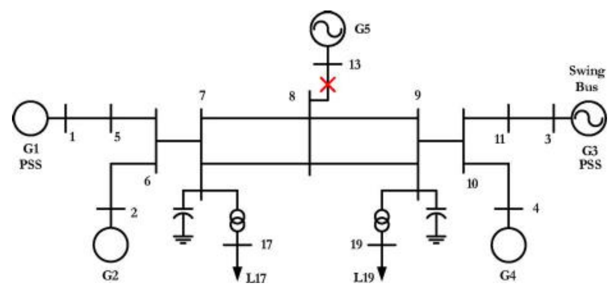

Fig. 2. KRK two-area system modified to include a small generator.

B. Small-Signal Analysis

In this paper we will demonstrate that the frequency response of a power system can be effectively studied using small-signal analysis tools along with conventional nonlinear dynamic simulation. A modified version of the Klein-Rogers-Kundur (KRK) two-area, four-generator system [32], [35] will be used as the test system. The linear analysis and nonlinear simulation are facilitated by the MATLAB-based Power System Toolbox (PST) software [36]. The linear model allows the use of the eigenvalues for tuning the frequency governing controllers and the eigenvectors for tracking the contents of the frequency regulation mode.

1) Test System Specifications: Fig. 2 depicts the KRK system used throughout this paper and Table II contains its load and generation specifications. The KRK system was modified to include a small Generator G5, on Bus 13, in the middle of the transfer path. The tripping of G5 is the loss of generation event. Because of its location, tripping G5 would not excite the interarea mode. In the test system, the power production in each area roughly equals its consumption making the power transfer between the areas significant only during disturbances.

This article has been accepted for inclusion in a future issue of this journal. Content is final as presented, with the exception of pagination.

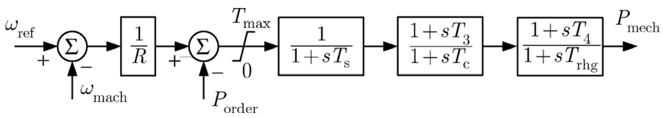

Fig. 3. Simple turbine governor model.

TABLE II
TEST SYSTEM GENERATOR AND LOAD DATA (BASE OF 100 MVA)

	P (pu)	Q (pu)	TG	Exc. ST3	PSS
G1	6.738	1.913	✓	✓	✓
G2	6.738	2.607	✓	✓	
G3	6.738	1.187	✓	✓	✓
G4	6.738	0.889	✓	✓	
G5	1.05	0.3751	✓	✓	
LOAD DATA					
	P (pu)	Q (pu)	%CPL	%CCL	%CIL
L17	13.67	1	20%	35%	45%
L19	13.67	1	20%	35%	45%

All five generators in this system are described by a subtransient model comprising 6 states. All generators are equipped with turbine governors shown in Fig. 3 modeled using 3 states, and Type-ST3 exciter [37] also defined by 3 states. Generators G1 and G3 at Buses 1 and 3, respectively, have PSS with 3 states each. Hence the total number of nonlinear differential equations of the system is 66. A modal analysis of the system consists of linearizing these differential equations with respect to the equilibrium operating point to obtain a linear system

$$\dot{\mathbf{x}} = \mathbf{A}\mathbf{x} + \mathbf{B}\mathbf{u}, \qquad \mathbf{y} = \mathbf{C}\mathbf{x} + \mathbf{D}\mathbf{u}. \tag{1}$$

For the test system, $\mathbf{A}$ is a matrix of dimension 66[1] and contains all the modal information of the system. Note that dead-bands in controllers are ignored in the linearization process.

Furthermore, in order to match the frequency response in Fig. 1, the loads L17 and L19 on Buses 17 and 19, respectively, have to be made sensitive to voltage and frequency. In this work, the frequency dependence component is ignored, as frequency variation of less than 0.02% is small. Because the actual bus voltages are computed, the loads are modeled with a combination of constant power (CPL), constant current (CCL), and constant impedance (CIL) as specified in Table II. Although the non-conforming loads do not require differential equations, the network solution has to be solved using iterations. With the chosen load composition values, the frequency response due to the loss-of-generation scenario is similar to the typical WECC frequency response presented in [30].

2) Test System Frequency Response Analysis: All the frequency response analyze in this paper are based on the following event: trip of Generator G5 at 0.5 s. This event implies a loss of about 3.75% of the total generation.

For this event we performed a study on how different generator parameters and load modeling characteristics affect the frequency response of the system and how they affect the modes

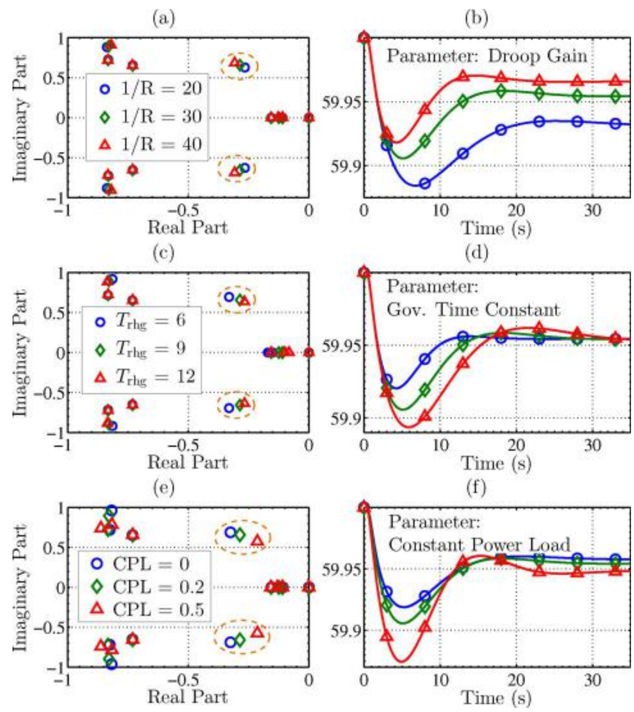

Fig. 4. Frequency response variations for synchronous machine parameter changes. (a) Poles of the systems. (b) System frequency (Hz). (c) Poles of the systems. (d) System frequency (Hz). (e) Poles of the systems. (f) System frequency (Hz).

of $\mathbf{A}$ (1). The left column of Fig. 4 show the eigenanalysis results as affected by –the droop gain of the governors, the speed at which the generator governors can act, and the sensitivities of the loads. This analysis shows that the eigenvalues that are most affected by these parameter changes are a complex pair at $-0.2859 \pm j0.6577$, a well-damped mode with a frequency of 0.1047 Hz. A participation factor calculation [38] shows that many states, include the generator speeds, turbine power fractions, and internal voltages[2] of all the machines, participate in this mode. Thus it is referred to as the *frequency regulation mode*. This mode is also impacted by the wind turbines participating in frequency control.

The results of the nonlinear simulation in the right columns in Fig. 4 are well known and are introduced here to show the linkage with those of the linearization in the right column. They show that both the frequency nadir and RoCoF are affected by these parameters. The settling frequency is not affected by the amount of inertia or the speed of the governing action, but it is affected by the governor droop gain as well as the load characteristics. Note that the responses shown in these plots are primarily due to the frequency regulation mode.

III. FREQUENCY RESPONSE FOR TEST SYSTEM WITH WIND GENERATION

In this section we will discuss how wind generation integration affects the frequency response of the test power system at 25% wind penetration.

[1]The system size is 54 when G5 is tripped. However, since G5 is small compared to the rest of the system, the modal property of (1) is largely preserved.

[2]The machine voltage variables participate in this mode because the power consumption of the loads is a function of the bus voltages.

This article has been accepted for inclusion in a future issue of this journal. Content is final as presented, with the exception of pagination.

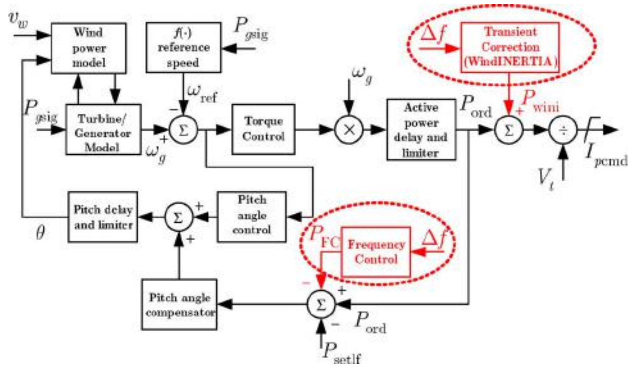

Fig. 5. Schematic diagram of the active power control part of the WTG models in [28] and [39]. The controllers proposed in this paper are shown inside the dashed lines.

A. WTG Model

The Type-3 doubly-fed asynchronous generator (DFAG) model is used for the wind turbine-generator (WTG) and implemented in PST [39]. It is a functional model that has been validated in previous works [40]–[44] and has been used extensively in wind studies [10], [12], [45], [46]. In this paper, individual wind turbines are lumped into a large aggregated wind turbine [28], [47]. Thus the impact of the wind turbine layout and the wind speed variations for individual wind turbines are not considered. The DFAG technology allows a wind turbine to operate at variable speed and respond to a time-varying wind profile as an input. The model also takes into consideration the physical limits of the machine such as the maximum and minimum pitch angle, power injection and their respective rates of change.

The power transfer of DFAGs occurs through power-electronics interfaces that can be modeled as a controlled current injection to the grid [28]. The power-electronics interface also allows the independent control of the active and reactive power current outputs from a DFAG.

Fig. 5 shows a simplified block diagram of the active power control of the WTG model [28]. The main inputs to this block are the wind profile ($v_w(t)$), the electrical power injected by the WTG (P_{gsig}), and the desired power output value P_{setlf}. The output is the desired active current injection I_{pcmd}. The active power control dynamics are determined mainly by three individual control functions, consisting of the following PI controllers:

$$\text{Pitch Control: } G_{\mathrm{cont}}(s) = K_{\mathrm{pp}} + \frac{K_{\mathrm{ip}}}{s} = 150 + \frac{25}{s} \quad (2)$$

$$\text{Pitch Comp. : } G_{\mathrm{comp}}(s) = K_{\mathrm{pc}} + \frac{K_{\mathrm{ic}}}{s} = 3 + \frac{30}{s} \quad (3)$$

$$\text{Torque Control : } G_{\mathrm{torq}}(s) = K_{\mathrm{ptrq}} + \frac{K_{\mathrm{itrq}}}{s} = 3 + \frac{0.6}{s}. \quad (4)$$

The control gain values in these equations are obtained from [28]. They will be used as the nominal values for design tuning. Note that the wind-up limits and filtering functions are not shown in these equations.

In this paper, the reactive power control of the WTG is assumed to regulate the terminal bus voltage.

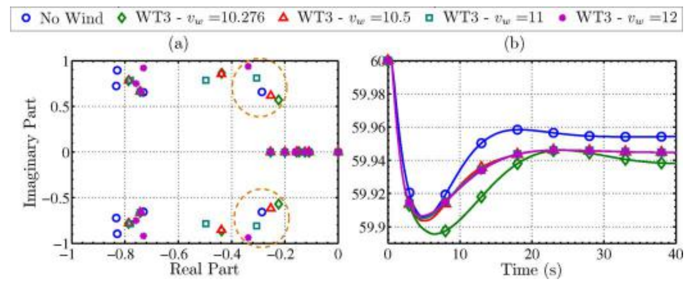

Fig. 6. Frequency response of the test system as affected by a wind penetration of 25%. (a) Poles of the systems. (b) System frequency (Hz).

B. Test System Simulations

In the 25% wind penetration scenario, Generator G4 is replaced by a Type-3 WTG of the same rating. The system now consists of 71 states of which 17 belong to the WTG. The WTG is subject to four different wind speeds, $v_w = 10.276$, 10.5, 11, and 12 m/s. The maximum power that can be extracted from these wind speeds exceeds 6.738 pu required for the WTG. As a result, the pitch angle is controlled to keep the additional available power as reserve.

Fig. 6(a) shows the variation of the frequency regulation mode for these different wind conditions, which indicates that the addition of the WTG changes moderately its damping and frequency. The loss-of-generator G5 event was simulated for the four wind conditions, and the time responses are shown in Fig. 6(b). At all wind velocities, the steady-state frequency regulation with the WTG is worse than the no-WTG system. At high wind speeds, the WTG is able to achieve the same level of nadir compared to the no-WTG system, due to the pitch-angle controller and the current injection interface.

IV. Proposed Frequency Control for WTG

This section investigates options of frequency control for WTGs and presents a new approach to achieve frequency control using the WTG Type-3 model described in Section III-A.

A. Enabling Frequency Response in WTGs

Frequency control during a loss of generation somewhere else in the system requires a WTG to provide additional electrical output power either in the short term (5–10 s) or for a longer term (30 s or more). There are two basic mechanisms to do so:

1) Operate the WTG in the conventional maximum energy capture mode and release energy stored in the WT rotor inertia should a frequency event occur: Because releasing inertia energy decreases the generator speed, a recovery period, in which the WTG produces less power than the nominal [13], is needed to restore the generator speed.[3] The recovery period does not appear in the case the WTG is operating at rated power with a high wind speed.
2) Operate the WTG in a deloaded manner: Deloading can be achieved by either operating the WTG at an suboptimal

[3]Note that WTGs cannot stably produce the same amount of energy if its speed is not restored to normal, as a lower speed translates into less mechanical power capture.

This article has been accepted for inclusion in a future issue of this journal. Content is final as presented, with the exception of pagination.

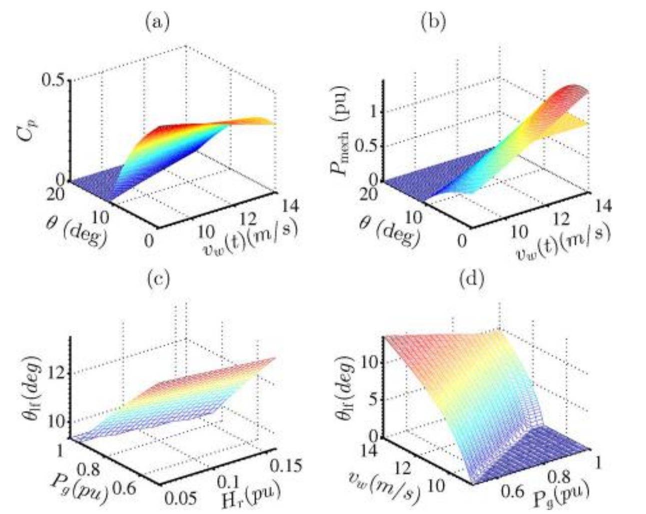

Fig. 7. Pitch angle and related functions. (a) C_p. (b) $P_{\rm mech} = P_g$. (c) $\theta_{\rm lf}$. (d) $\theta_{\rm lf}$.

generator speed or pitching the blade angle to intentionally spill power, so that the reserve energy can be used for frequency regulation. This paper investigates the latter option of controlling the pitch angle to respond to system frequency changes, using an optimal generator speed determined by [28]

$$\omega_{\rm ref} = \begin{cases} -0.75P_g^2 + 1.59P_g + 0.63, & \text{if } P_g < 0.46 \\ 1.2, & \text{if } P_g \geq 0.46 \end{cases} \quad (5)$$

where P_g corresponds to the output power of the WTG. In the context of the proposed design when the WTG is operating at a high power level, $\omega_{\rm ref}$ is kept at 1.2 pu.

The proposed pitch angle control modifies the setpoint value of $P_{\rm setlf}$ (or $P_{\rm rated}$) to match the power output as required by the power flow solution (corresponding to P_g). The controlled pitch angle is moved from $\theta_{\min} = 0$ to

$$\theta_{\rm lf} = f_\theta(P_g, H_r, v_w) > 0 \quad (6)$$

where P_g is the WTG output power, H_r is the desired power headroom, and v_w is the wind speed input of the WT. The function f is built on the wind capacity function C_p [Fig. 7(a)] and the power captured from wind by the WT [Fig. 7(b)]

$$P_{\rm mech} = K_p C_p(\lambda(v_w, \omega_t), \theta) v_w^3 \quad (7)$$

by setting

$$P_g(1 + H_r) = P_{\rm mech} \quad (8)$$

and $\theta = 0$, a minimum wind speed $v_{w\min}$ to provide the desired headroom is determined. If the wind profile is above $v_{w\min}$, $\theta_{\rm lf}$ can be determined using again (7) but with $P_{\rm mech} = P_g$ and the actual wind speed v_w.

B. Governing Control

In a deloaded mode, the pitch angle of a WTG is made to respond to frequency variations, akin to the governing function in conventional steam and hydro turbines. A proportional control structure shown in Fig. 8 is used to generate an supplemental

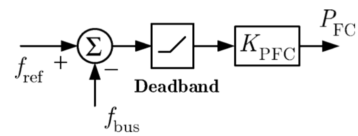

Fig. 8. Proportional control to enable frequency response in WTG.

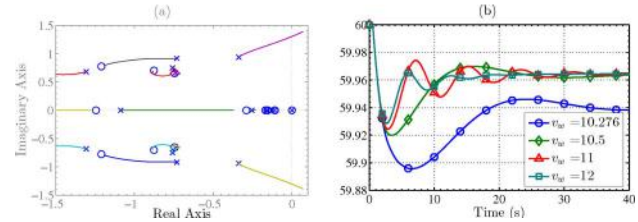

Fig. 9. Root Locus and time responses for proportional frequency control. (a) Root locus $- v_w = 12$ m/s. (b) System frequency (Hz).

power order $P_{\rm FC}$. The purpose of the deadband in Fig. 8 is twofold: first, it prevents the control from acting on small fluctuations (noise) and second, it makes the controller unresponsive to excess of generation events as these are less problematic when connecting wind into the system. This controller needs to be integrated into the existing WTG control without changing the structure of the multiple PI controllers, although the tuning of the PI controller gains may be necessary.

1) Controller Structure and Implementation: As shown in Fig. 5, the electric output power $P_{\rm ord}$ is set to follow the dispatched power setpoint ($P_{\rm setlf}$). Thus the supplemental control signal $P_{\rm FC}$ that is responsive to the frequency deviation should be added to ($P_{\rm setlf}$), as shown in Fig. 5. Adding $P_{\rm FC}$ to any other injection points in the control diagram will result in the integrators in the controller blocks (2)–(4) cancelling out the effect of $P_{\rm FC}$ in steady state. This implementation will add to the pitch compensation of (3), and will guarantee modifications in the mechanical power captured from the wind to provide additional $P_{\rm ord}$. In cases when the frequency deviation is high, the integrator in the pitch compensator will be limited by the wind-up limit once the pitch angle reaches zero.

Fig. 9(b) shows the frequency regulation for the 25% wind penetration scenario described in Section III-B, when the proposed controller ($K_{\rm PFC} = 60$) has been implemented in the WTG at Bus 4. The gain $K_{\rm PFC} = 60$ is chosen to ensure that the WTG participates strongly in frequency regulation after the trip of Generator G5. The results show a clear improvement in the frequency nadir and settling frequency compared to the case the WTG is not regulating frequency ($v_w = 10.276$ m/s). However the simulation also shows that low frequency oscillations of the power system appear as the wind speed, and hence the headroom, is increased. This behavior is confirmed by a root-locus analysis shown in Fig. 9(a) that when $K_{\rm PFC}$ increases the *frequency regulation mode* moves towards instability.

Attempts to improve the damping of the frequency regulation mode by adding phase compensation (like in PSS design) to the controller in Fig. 8 were not successful, as the design impacted unfavorably the interarea mode (located at $-0.276 \pm j3.49$) of the KRK system. As a result, the impact of the control gain parameters of the 3 PI controllers (2)–(4) on the frequency regulation mode is investigated.

This article has been accepted for inclusion in a future issue of this journal. Content is final as presented, with the exception of pagination.

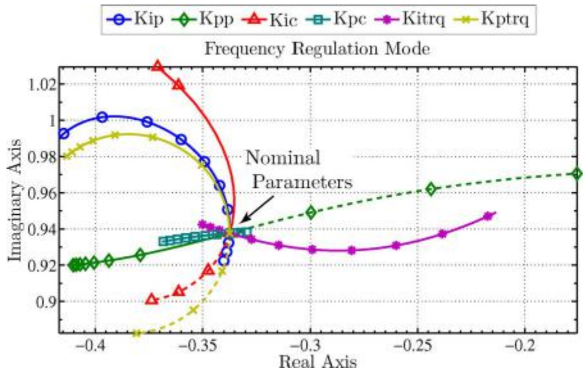

Fig. 10. Frequency regulation mode variations for changes in different WTG control parameters. Solid lines indicate the variation when the parameter is increased while dashed lines show the variations when it is decreased.

TABLE III
WTG Control Parameters Specifications in Fig. 10

Parameter		Value		
		Nominal	Initial	Final
Pitch Control	K_{ip}	25	12	100
	K_{pp}	150	75	600
Pitch Compensation	K_{ic}	30	15	45
	K_{pc}	3	1.5	12
Torque Control	K_{itrq}	0.6	0.2	2.4
	K_{ptrq}	3	1.5	12

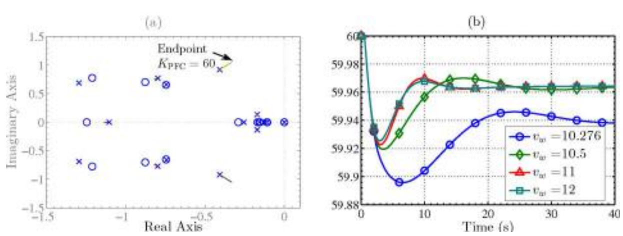

Fig. 11. Root Locus and time responses for proportional frequency control for the pitch control proportional constant $K_{\text{pp}} = 450$. (a) Root locus $- v_w = 12$ m/s. (b) System frequency (Hz).

2) WTG Control Model Parameter Adjustment: The design idea is to perform a sensitivity analysis on the control parameters of the WTG[4] to check whether they can be changed to improve the damping of the frequency regulation mode. Fig. 10 is a root-locus plot showing the impact of varying the integral and proportional control parameters in (2)–(4) on the frequency regulation mode. The starting and ending values of these parameters are shown in Table III. The results suggest that increasing only the proportional constant K_{pp} will suffice to improve sufficiently the damping on the frequency regulation mode.

Fig. 11(b) shows the results for the same scenario as that of Fig. 9(b) but with $K_{\text{pp}} = 450$. The simulation shows that the oscillation due to the frequency regulation mode is no longer present at high wind speed conditions. Fig. 11(a) indicates a reduction of the sensitivity of the frequency regulation mode to the proposed frequency control gain.

[4]This aspect for a subset of control parameters was investigated in [10] via time simulation.

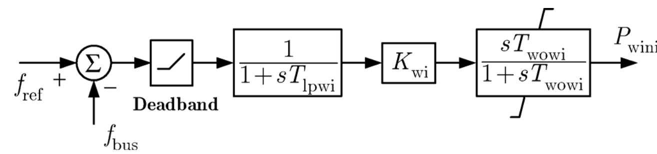

Fig. 12. WindINERTIA like control diagram.

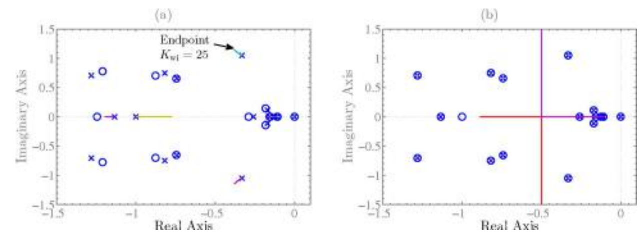

Fig. 13. Frequency regulation mode as affected by the transient correction parameters K_{wi} and T_{wowi}. (a) Root locus—parameter K_{wi}. (b) Root locus—parameter T_{wowi}.

TABLE IV
Proposed and GE Recommended WindINERTIA Parameters

Parameter	Values	
	Proposed	GE Recommended
K_{itrq}	0.6	0.05
K_{ptrq}	3	0.5
T_{pc}	0.05	4.0
K_{wi}	25	10
T_{wowi}	7.5	5.5

C. Wind Inertia Control

The main purpose of the K_{PFC} controller is to improve the steady-state frequency response, although it offers some benefit in improving the frequency nadir. To further improve the frequency nadir (and RoCoF) of the system, it is desirable to add a transient frequency response controller that would not adversely affect K_{PFC}. The design idea is to introduce a rate control which will respond quickly to frequency variation. To this end, the control structure of the WindINERTIA control proposed for GE Type-3 WTGs is adopted (Fig. 12). Note that in steady state, this controller will not be active. Thus it is appropriate to add this control signal to the P_{ord} injection point, as shown in Fig. 5, because in this configuration, the WTG will boost its power output immediately. Although the controller structure is not new, a contribution of this paper is to show that the wind inertia controller design can be established via a root-locus analysis.

The differences between the gains of the proposed wind inertia controller and WindINERTIA in [28] are summarized in Table IV. The proposed control does not further modify any control parameter of the model: it keeps the modification on K_{pp} in place whereas WindINERTIA [28] requires the modification of K_{itrq}, K_{ptrq}, T_{pc}. Parameter K_{wi} is increased so the WTG responds faster to drops in frequency to mitigate the initial frequency drop, and the washout time constant T_{wowi} is slightly increased. Fig. 13 demonstrates that the proposed transient control configuration does not alter the stability of the system as the frequency regulation mode is hardly affected by K_{wi} or T_{wowi}. Note that the system now has 73 states as the wind inertia controller is described by 2 states.

This article has been accepted for inclusion in a future issue of this journal. Content is final as presented, with the exception of pagination.

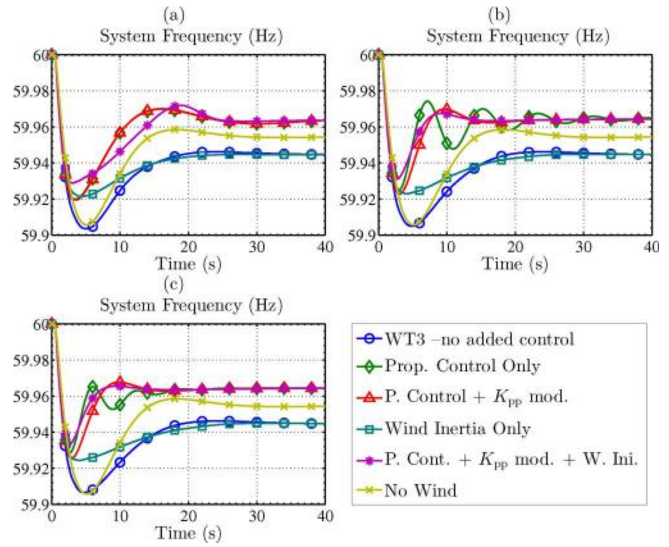

Fig. 14. Comparison between different frequency control schemes for different wind speeds. (a) $v_w = 10.5$ m/s. (b) $v_w = 11$ m/s. (c) $v_w = 12$ m/s.

TABLE V
FREQUENCY RESPONSE COMPARISON AT $v_w = 11$ m/s

Case	Freq. Nadir (Hz)	Settling Freq. (Hz)	RoCoF (Hz/s)
No Wind	59.9057	59.9543	-0.0444
WT3 –no added control	59.905	59.9447	-0.0588
K_{PFC} Only	59.9244	59.9643	-0.0587
K_{PFC} + K_{pp} modification	59.9228	59.9644	-0.0587
Wind Inertia Only	59.9229	59.9447	-0.0577
K_{PFC} + K_{pp} mod. + W. Ini.	59.9308	59.9644	-0.0576

D. 25% of Wind Penetration Control Comparison

The test system with 25% wind generation penetration, where a Type-3 WTG is connected at Bus 4, is simulated for the trip of Generator G5 event to illustrate the various control designs proposed in this paper. The results presented in Fig. 14 and summarized in Table V indicate that regulating frequency with WTG is possible by using a properly tuned proportional control. They further show that the wind inertia controller in Section IV-C clearly helps with the frequency nadir.

V. INCREASED WIND PENETRATION

This section shows the application of the proposed control design to the test system with 50% wind generation penetration, in which Generators G2 and G4 are substituted by Type-3 WTGs of the same rating. This modification implies that wind generation produces roughly half of the power in each area. This configuration allows the evaluation of potential controller interactions on multiple WTGs. The system now consists of 76 states, not including the proposed frequency controllers implemented in the WTGs.

A. 50% Wind Penetration Analysis

Fig. 15 shows the impact on the frequency regulation mode from the WTG in Area 1 (at Bus 2) and in Area 2 (at Bus 4) independently (for 25% penetration) and together (for 50% penetration). It also shows the damping improvement by increasing K_{pp} for all cases including the 50% wind generation case.

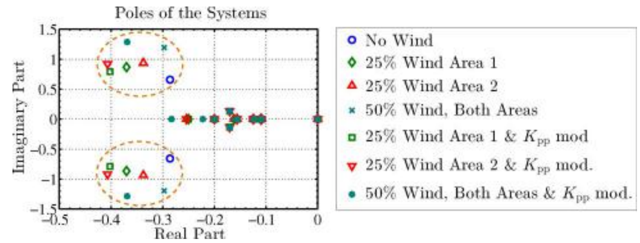

Fig. 15. Effect of integrating wind up to 50% in the frequency regulation mode.

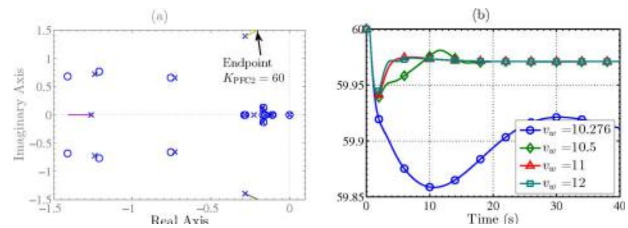

Fig. 16. (a) Root Locus plot for the WTG in Area 2 with the WTG in Area 1 enabled with the proposed frequency control ($K_{PFC1} = 60$). (b) Proposed frequency control scheme for different wind speeds at 50% wind penetration. (a) Root locus—WTG in Area 2. (b) System frequency (Hz).

Fig. 16(a) shows the impact of the proposed proportional frequency control on the WTG in Area 2 on the frequency regulation mode when the proposed controller is already implemented on the WTG in Area 1. Clearly the addition of the two controllers does not significantly alter the mode. The loss-of-generator G5 was simulated for the four wind conditions and the results are shown in Fig. 16(b). The wind condition $v_w = 10.276$ m/s is the base case where the WTG is unresponsive to frequency. A comparison between this case and the other cases clearly shows an improvement both in the nadir and the settling frequency.

It can be deduced from the results presented in this section and those in Figs. 11 and 14 that a higher wind penetration yields a more responsive frequency regulation of the system, provided that the wind generation is equipped with the proposed governing function. This is in part because the inverter-based interfaces of WTG are more flexible and can respond quicker than conventional generation [48].

B. Loss of Wind Generation due to Wind Speed Drop

In addition, for the 50% wind scenario, the responsiveness of the proposed control to wind variation is illustrated. Consider the case of dropping the wind velocity from 12 m/s to 9.8 m/s for the WTG G4 in Area 2. In such a scenario, G4 reduces its pitch angle to 0° and its power to 6.02 pu, a reduction of almost 8%. The resulting simulation in Fig. 17, shows that the other WTG G2 with the proposed frequency control enabled, along with the remaining conventional generation, is able to minimize the frequency deviations in this disturbance.

C. Variable Wind Speed Case

To further demonstrate the effectiveness of the proposed control, a case where the wind speed is variable for both wind units

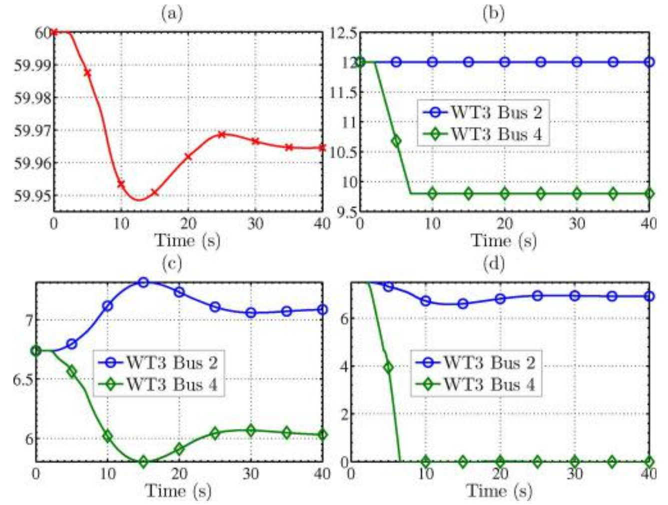

Fig. 17. Proposed frequency control scheme at 50% wind penetration when a loss of wind power occurs in G4. (a) System frequency (Hz). (b) Wind speed (m/s). (c) Power injection by WTGs (pu). (d) Pitch angle (deg).

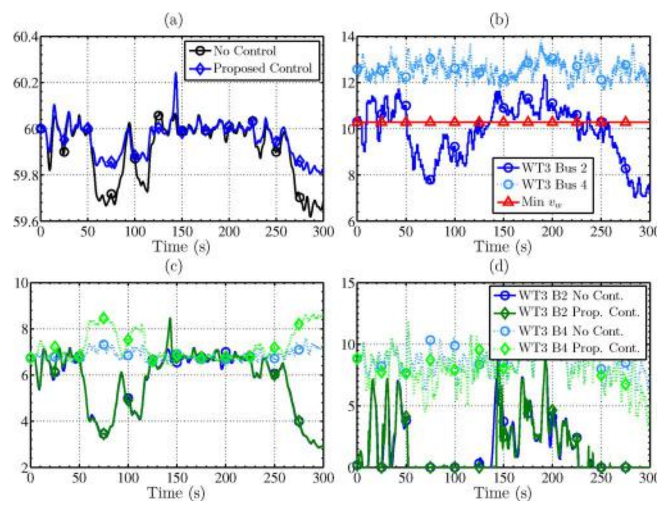

Fig. 18. Comparison between the proposed frequency control scheme and WT without frequency control at 50% wind penetration for a non constant (measured) wind speed as input for the wind generators. (a) System frequency (Hz). (b) Wind speed (m/s). (c) Power injection by WTGs (pu). (d) Pitch angle (deg).

is considered. The time-varying wind profile for the WTG at Bus 2 corresponds to a 5-min wind speed measurement while the wind input for the WTG at Bus 4 is a simulated wind profile that follows a Weibull distribution [49] (with shape parameter k $= 1.9541$ and scale parameter $c = 9.1251$). Both of these wind inputs are shown in Fig. 18(b). Fig. 18(a) shows the frequency response of the system for the case where the WTGs have no frequency control and the case where both WTGs have the proposed control. This figure shows that the frequency drops occurring in the system due to wind speed variations are reduced by the inclusion of the proposed control. In particular, the maximum frequency drop occurring in the system during the interval of 50 and 125 s is improved from 59.67 Hz to 59.86 Hz as the adjustment of the pitch angle [Fig. 18(a)] increases the power level [Fig. 18(c)]. In general, The frequency of the system with the WTGs participating in frequency response is closer to the nominal value than the case without frequency governing. Note that the motion of the pitch angles in Figs. 17(d) and 18(d) are within the $10°/s$ capability [28].

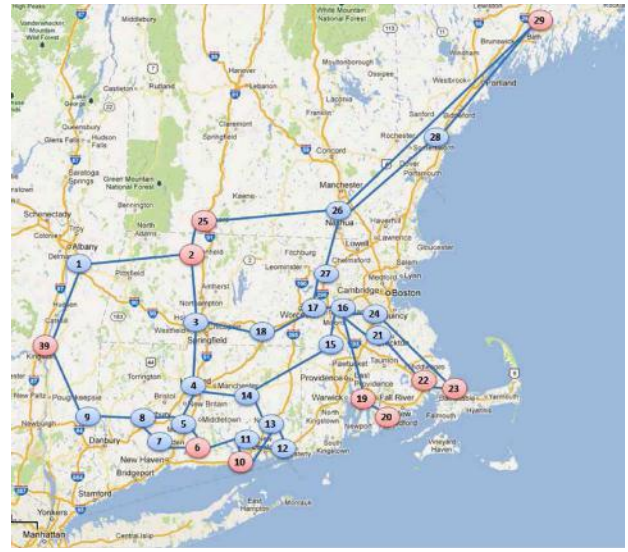

Fig. 19. Map of the 39-bus, 10-machine New-England reduced system. The data for this system can be found in [50].

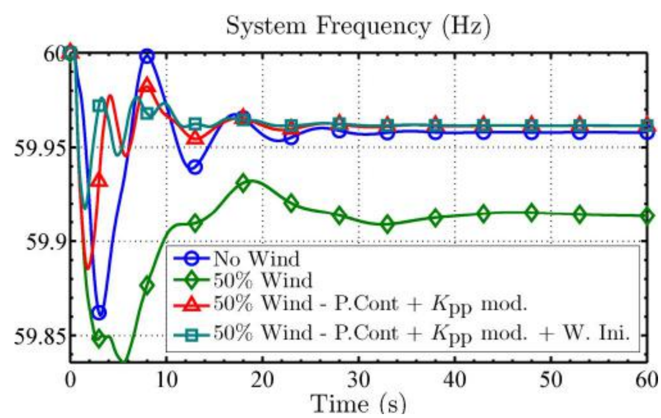

Fig. 20. Frequency responses for the New England 10-machine system.

D. New England 10-Generator System

A reduced New England system shown in Fig. 19 is used to illustrate the performance of the proposed wind turbine frequency regulation in a larger system. This system has 39 buses and 10 generating units [50]. The total generation of the system is around 62 pu, in a base of 100 MVA, and the loss of generation event is the trip of the generator at Bus 2, which represents a loss of about 4% of the total generation.

To achieve 50% of wind penetration the synchronous machines at Buses 10, 19, 20, 22, and 23 were replaced by WTGs of the same size. Four cases to study the frequency response of the system were considered. The first, in Fig. 20 (blue), is the system without wind turbines and shows a response similar to recorded unit trip events in New England [51]. The second case, in Fig. 20 (green), shows the response of the system at 50% wind penetration when the wind units are not responsive to frequency fluctuations. Note that at this conditions the frequency response of the system is greatly deteriorated. Fig. 20 (red) shows the third case in which the proposed steady-state frequency control was included on all 5 WTGs. Note that the frequency response performance of the system is restored. In fact, the frequency nadir is improved and the settling frequency is slightly higher than that in the no wind-turbine system. For this case the gain K_{PFC} was adjusted to 25 to both achieve a reasonable settling frequency value and reduce the natural oscillations of the remaining generators of the system. Finally, the case in Fig. 20 (cyan) shows the frequency response of the system when the proposed controller, including the transient part of inertia emulation control, is included in the WTGs of the system. For this case it is observed that the transient controller objective is accomplished because the frequency nadir performance of the system is further improved.

VI. Conclusions

This paper analyzes how integrating Type-3 WTG affects the system frequency response of a test power system. The analysis presented are performed using a realistic production grade WTG model [28]. It shows that integrating wind generation without frequency control deteriorates the frequency response and that the frequency regulation of this test system is mainly determined by the frequency-regulation mode, which is affected by wind integration.

A control to mitigate the effects of wind integration on system frequency response is proposed. The control requires operating the WTG in a deloaded manner through blade pitching. Root-locus analyses based on small-signal models provide the insight in control parameter tuning to achieve a stable controller design. Results presented in this paper indicate that including proper frequency regulation controls in wind generation improves considerably the frequency response of the system. This is due to the fact that wind generation interfaces with the grid through power electronics, allowing a faster and more flexible control of the power output. The paper hence provides a pathway for WTG to provide frequency response should they are required to do so. The results of this paper are further validated in a larger system with 10 generating units.

Future work will include evaluating the effects of integrating Type-4 WTG on a power system and comparing them with the design results of Type-3 WTGs. Higher values of wind penetration will also be tested. In addition, the implementation of the control on individual wind turbines, including considerations of communication schemes, need to be investigated.

References

[1] R. Wiser and M. Bolinger, "2013 Wind Technologies Market Report," Tech. Rep., United States Department of Energy, 2014.

[2] "Global Wind Report, Annual Market Update," Tech. Rep., Global Wind Energy Council, 2014.

[3] "NERC IVGTF Task 2.4 Report- Operating Practices, Procedures, and Tools," NERC, Tech. Rep., NERC, 2011.

[4] A. Mullane and M. O'Malley, "The inertial response of induction-machine-based wind turbines," *IEEE Trans. Power Syst.*, vol. 20, no. 3, pp. 1496–1503, Aug. 2005.

[5] J. Ekanayake and N. Jenkins, "Comparison of the response of doubly fed and fixed-speed induction generator wind turbines to changes in network frequency," *IEEE Trans. Energy Convers.*, vol. 19, no. 4, pp. 800–802, Dec. 2004.

[6] J. Morren, S. W. De Haan, W. L. Kling, and J. Ferreira, "Wind turbines emulating inertia and supporting primary frequency control," *IEEE Trans. Power Syst.*, vol. 21, no. 1, pp. 433–434, Feb. 2006.

[7] J. M. Mauricio, A. Marano, A. Gómez-Expósito, and J. L. Martinez-Ramos, "Frequency regulation contribution through variable-speed wind energy conversion systems," *IEEE Trans. Power Syst.*, vol. 24, no. 1, pp. 173–180, Feb. 2009.

[8] G. Lalor, A. Mullane, and M. O'Malley, "Frequency control and wind turbine technologies," *IEEE Trans. Power Syst.*, vol. 20, no. 4, pp. 1905–1913, Nov. 2005.

[9] M. Kayikçi and J. V. Milanović, "Dynamic contribution of DFIG-based wind plants to system frequency disturbances," *IEEE Trans. Power Syst.*, vol. 24, no. 2, pp. 859–867, May 2009.

[10] D. Gautam, L. Goel, R. Ayyanar, V. Vittal, and T. Harbour, "Control strategy to mitigate the impact of reduced inertia due to doubly fed induction generators on large power systems," *IEEE Trans. Power Syst.*, vol. 26, no. 1, pp. 214–224, Feb. 2011.

[11] A. Mullane and M. O'Malley, "Modifying the inertial response of power-converter based wind turbine generators," in *Proc. 3rd IET Int. Conf. Power Electronics, Machines and Drives*, 2006.

[12] L. N. Papangelis and C. D. Vournas, "Design principles of wind turbine inertia emulators for autonomous systems," in *Preprints 19th World Congr.*, 2014, pp. 5844–5851.

[13] J. Aho, A. Buckspan, J. Laks, P. Fleming, Y. Jeong, F. Dunne, M. Churchfield, L. Pao, and K. Johnson, "A tutorial of wind turbine control for supporting grid frequency through active power control," in *Proc. Amer. Control Conf. (ACC), 2012*, 2012, pp. 3120–3131.

[14] L. Holdsworth, J. Ekanayake, and N. Jenkins, "Power system frequency response from fixed speed and doubly fed induction generator-based wind turbines," *Wind Energy*, vol. 7, no. 1, pp. 21–35, 2004.

[15] R. G. De Almeida and J. A. Peças Lopes, "Participation of doubly fed induction wind generators in system frequency regulation," *IEEE Trans. Power Syst.*, vol. 22, no. 3, pp. 944–950, Aug. 2007.

[16] E. Loukarakis, I. Margaris, and P. Moutis, "Frequency control support and participation methods provided by wind generation," in *Proc. 2009 IEEE Electrical Power & Energy Conf. (EPEC)*, 2009, pp. 1–6.

[17] E. Muljadi, V. Gevorgian, M. Singh, and S. Santoso, "Understanding inertial and frequency response of wind power plants," in *Proc. IEEE Symp. Power Electronics and Electric Machines in Wind Applications*, 2012, pp. 1–8.

[18] B. H. Chowdhury and H. T. Ma, "Frequency regulation with wind power plants," in *Proc. 2008 IEEE Power and Energy Soc. General Meeting—Conversion and Delivery of Electrical Energy in the 21st Century*, 2008, pp. 1–5.

[19] P.-K. Keung, P. Li, H. Banakar, and B. T. Ooi, "Kinetic energy of wind-turbine generators for system frequency support," *IEEE Trans. Power Syst.*, vol. 24, no. 1, pp. 279–287, Feb. 2009.

[20] G. Ramtharan, N. Jenkins, and J. Ekanayake, "Frequency support from doubly fed induction generator wind turbines," *IET Renew. Power Gener.*, vol. 1, no. 1, pp. 3–9, 2007.

[21] A. Teninge, C. Jecu, D. Roye, S. Bacha, J. Duval, and R. Belhomme, "Contribution to frequency control through wind turbine inertial energy storage," *IET Renew. Power Gener.*, vol. 3, no. 3, pp. 358–370, 2009.

[22] I. Erlich and M. Wilch, "Primary frequency control by wind turbines," in *Proc. 2010 IEEE Power and Energy Soc. General Meeting*, 2010, pp. 1–8.

[23] ERCOT Nodal Protocols April 2, 2013, ERCOT.

[24] Wind Turbines Connected to Grids with Voltages Above 100 KV -Technical Regulation for the Properties and the Regulation of Wind Turbines, Elkraft System and Eltra Regulation, 2004.

[25] E. Fagan, S. Grimes, J. McArdle, P. Smith, and M. Stronge, "Grid code provisions for wind generators in ireland," in *Proc. 2005 IEEE Power Eng. Soc. General Meeting*, 2005, pp. 1241–1247.

[26] M. Altın, O. Goksu, R. Teodorescu, P. Rodriguez, B.-B. Jensen, and L. Helle, "Overview of recent grid codes for wind power integration," in *Proc. 2010 12th Int. Conf. Optimization of Electrical and Electron. Equipment (OPTIM)*, 2010, pp. 1152–1160.

[27] B. Kirby, M. Milligan, and E. Ela, "Providing minute-to-minute regulation from wind plants," in *Proc. 9th Annu. Large-Scale Integration of Wind Power into Power Systems and Transmission Networks for Offshore Wind Power Plant*, 2010.

[28] M. Shao, N. Miller, J. Sanchez-Gasca, and J. MacDowell, "Modeling of GE Wind Turbine-Generator for Grid Studies, Version 4.6," Tech. Rep., General Electric International, Inc., 2013.

[29] Y. Wang, G. Delille, H. Bayem, X. Guillaud, and B. Francois, "High wind power penetration in isolated power systems–Assessment of wind inertial and primary frequency responses," *IEEE Trans. Power Syst.*, vol. 28, no. 3, pp. 2412–2420, Aug. 2013.

[30] "Balancing and Frequency Control: A Technical Document Prepared by the NERC Resources Subcommittee," NERC, Tech. Rep., NERC, 2011.

[31] Rate of Change of Frequency DS3 Advisory Council Discussion Paper, EIRGRID and SoNi, 2013.

[32] P. Kundur, *Power System Stability and Control*. New York, NY, USA: McGraw-Hill, 1994, vol. 7.

[33] J. W. Ingleson and E. Allen, "Tracking the Eastern interconnection frequency governing characteristic," in *Proc. 2010 IEEE Power and Energy Soc. General Meeting*, 2010, pp. 1–6.

[34] S. Sharma, S.-H. Huang, and N. D. R. Sarma, "System inertial frequency response estimation and impact of renewable resources in ERCOT interconnection," in *Proc. 2011 IEEE Power and Energy Soc. General Meeting*, 2011, pp. 1–6.

[35] M. Klein, G. J. Rogers, and P. Kundur, "A fundamental study of inter-area oscillations in power systems," *IEEE Trans. Power Syst.*, vol. 6, no. 3, pp. 914–921, Aug. 1991.

[36] J. H. Chow and K. W. Cheung, "A Toolbox for power system dynamics and control engineering education and research," *IEEE Trans. Power Syst.*, vol. 7, no. 4, pp. 1559–1564, Nov. 1992.

[37] IEEE Committee Report, "Excitation system models for power system stability studies," *IEEE Trans. Power App. Syst.*, vol. PAS-100, no. 2, pp. 494–509, Feb. 1981.

[38] I. J. Pérez-Arriaga, G. C. Verghese, and F. C. Schweppe, "Selective modal analysis with applications to electric power systems, Part I: Heuristic introduction," *IEEE Trans. Power App. Syst.*, vol. PAS-101, no. 9, pp. 3117–3125, Sep. 1982.

[39] F. Wilches-Bernal, J. J. Sanchez-Gasca, and J. H. Chow, "Implementation of wind turbine generator models in the power system Toolbox," in *Proc. 2014 IEEE Power and Energy Conf. Illinois (PECI)*, 2014, pp. 1–5.

[40] N. Miller, J. MacDowell, G. Chmiel, R. Konopinski, D. Gautam, G. Laughter, and D. Hagen, "Coordinated voltage control for multiple wind plants in Eastern Wyoming: Analysis and field experience," in *Proc. 2012 IEEE Power Electron. and Machines in Wind Applicat. (PEMWA)*, 2012, pp. 1–8.

[41] J. M. MacDowell, K. Clark, N. W. Miller, and J. J. Sanchez-Gasca, "Validation of GE wind plant models for system planning simulations," in *Proc. 2011 IEEE Power and Energy Soc. General Meeting*, 2011, pp. 1–8.

[42] N. Miller, R. Delmerico, K. Kuruvilla, and M. Shao, "Frequency responsive controls for wind plants in grids with wind high penetration," in *Proc. 2012 IEEE Power and Energy Soc. General Meeting*, 2012, pp. 1–7.

[43] N. Miller, M. Shao, S. Pajic, and R. D'Aquila, *"Eastern Frequency Response Study," Tech. Rep.*. Golden, CO, USA: National Renewable Energy Laboratory (NREL), 2013.

[44] M. Asmine *et al.*, "Model validation for wind turbine generator models," *IEEE Trans. Power Syst.*, vol. 26, no. 3, pp. 1769–1782, Aug. 2011.

[45] N. Miller, K. Clark, and M. Shao, "Frequency responsive wind plant controls: Impacts on grid performance," in *Proc. 2011 IEEE Power and Energy Soc. General Meeting*, 2011, pp. 1–8.

[46] G. Tsourakis, B. Nomikos, and C. Vournas, "Effect of wind parks with doubly fed asynchronous generators on small-signal stability," *Electr. Power Syst. Res.*, vol. 79, no. 1, pp. 190–200, 2009.

[47] Modeling and Dynamic Behavior of Wind Generation as it Relates to Power System Control and Dynamic Performance, CIGRE WG C4.601, 2007, CIGRE Tech. Brochure 318.

[48] N. Miller, M. Shao, S. Pajic, and R. D'Aquila, "Wind and Solar Integration Study Phase 3 -Frequency Response and Transient Stability," Tech. Rep., GE Energy Management prepared for NREL, 2014.

[49] R. Kollu, S. R. Rayapudi, S. Narasimham, and K. M. Pakkurthi, "Mixture probability distribution functions to model wind speed distributions," *Int. J. Energy Environ. Eng.*, vol. 3, no. 1, p. 27, 2012.

[50] J. H. Chow, K. W. Cheung, and G. Rogers, Power System Toolbox Webpage [Online]. Available: http://www.eps.ee.kth.se/personal/luigiv/pst/Power_System_Toolbox_Webpage/PST.html

[51] A. Bykhovsky and J. H. Chow, "Power system disturbance identification from recorded dynamic data at the Northfield substation," *Int. J. Electr. Power Energy Syst.*, vol. 25, no. 10, pp. 787–795, 2003.

Felipe Wilches-Bernal (S'12) received the B.S. degree in electrical engineering from Universidad Javeriana, Bogotá, Colombia, and the M.S. degree in control systems and signal processing from Université Paris-Sud XI, Orsay, France. He is currently pursuing the Ph.D. degree in electrical engineering at Rensselaer Polytechnic Institute, Troy, NY, USA.

His research interest include power system stability and control, renewable energy and smart grid technologies, and signal processing and control techniques applied to power systems.

Joe H. Chow (F'92) received the M.S. and Ph.D. degrees from the University of Illinois, Urbana-Champaign, Urbana, IL, USA.

After working in the General Electric power system business in Schenectady, NY, USA, he joined Rensselaer Polytechnic Institute, Troy, NY, USA, in 1987, where he is a Professor of Electrical, Computer, and Systems Engineering. His research interests include power system dynamics and control, synchronized phasor data, and renewable generation.

Juan J. Sanchez-Gasca (F'02) received the M.S. and Ph.D. degrees from the University of Wisconsin-Madison, Madison, WI, USA.

He is with GE Energy Consulting, Schenectady, NY, USA. His work is related to different aspects of power system dynamics including the implementation of wind turbine generator models in GE's transient stability program.